

# Characterization of DNA Adducts Derived from syn-Benzo[ghi]fluoranthene-3,4-dihydrodiol-5,5a-epoxide and Comparative DNA Binding Studies with Structurally-Related anti-Diolepoxides of Benzo[ghi]fluoranthene and Benzo[c]phenanthrene

Hui-Fang Chang,<sup>†</sup> Duane M. Huffer,<sup>‡</sup> M. Paul Chiarelli,<sup>‡</sup> Lonnie R. Blankenship,<sup>§</sup> Sandra J. Culp,<sup>§</sup> and Bongsup P. Cho<sup>\*,†</sup>

Department of Biomedical Sciences, University of Rhode Island, Kingston, Rhode Island 02881, Department of Chemistry, Loyola University, Chicago, Illinois 60626, and Division of Biochemical Toxicology, National Center for Toxicological Research, Jefferson, Arkansas 72079

Received August 9, 2001

This paper reports structural characterization of the adducts and tetraols formed from syn-benzo[ghi]fluoranthene-3,4-dihydrodiol-5,5a-epoxide (syn-B[ghi]FDE, **3**) and comparative DNA-binding and mutagenicity studies involving **3**, anti-B[ghi]FDE (**2**), and anti-benzo[c]phenanthrene-11,12-dihydrodiol-13,14-epoxide (anti-BcPDE, **5**). The structures of nine DNA adducts and two racemic tetraols derived from **3** have been determined spectroscopically. Similar characterization of adducts obtained from the anti-isomer **2** was described in the preceding paper in this issue [Chang et al. (2002) *Chem. Res. Toxicol.* **15**, 187–197]. The majority of DNA adducts with **3** are those from the trans- or cis-opening of the epoxide at C5a by the exocyclic amino groups of dG, dA, and dC. The diolepoxides **2** and **3** are rigid structure analogues of anti- and syn-BcPDE (**5** and **6**), respectively, thus serving as models for probing molecular deformity and diol conformation in diolepoxide–DNA interaction. Comparative DNA binding experiments indicate that 57% of **2** and 33% of **3** were converted into DNA adducts, whereas a 71% conversion was observed for **5**. In general, lower percentages were observed with denatured calf-thymus DNA. As for base selectivity, **2** showed a greater affinity for dA relative to dG (dA/dG ratio, 0.79) than **3** (0.56) when reacted with native calf-thymus DNA. A much higher dA/dG ratio (1.41) was obtained for **5**. The overall dA/dG ratios were lower with denatured DNA, indicating the importance of the secondary structure of DNA for both adduct formation and chemical selectivity. The T-shape pseudo-diaxial diols of **3** appears to have favorable electrostatic interactions with the nearby phosphate backbone in the minor groove of DNA, thereby yielding greater amounts of dG adducts than the pseudo-diequatorial **2**. The anti-isomer **2** was found to be seven times more mutagenic than **3**, but they are significantly less mutagenic than the nonplanar analogue **5** when tested in *Salmonella typhimurium* TA 100.

## Introduction

Polycyclic aromatic hydrocarbons (PAHs)<sup>1</sup> are important environmental carcinogens (*1*, *2*). The structure–function–relationships of PAHs have been studied extensively over the past several decades; however, many fine structural and mechanical details regarding the interactions of PAH diolepoxides with DNA at the molecular-genetic level are beginning to emerge only recently (*3–8*). A recent surge of interest in PAH research is due primarily to the findings that the diolepoxides derived from sterically hindered fjord-region PAHs, such as benzo[c]phenanthrene, 5,6-dimethylchrysene, and dibenzo[a,l]pyrene, are exceptionally mutagenic and tumorigenic and exhibit unusually higher DNA adduct formations and greater binding affinity to dA over dG than

those derived from the less-hindered analogues, such as chrysene and benzo[a]pyrene (*9–18*). The substantial amount of data accumulated thus far indicates that activity increases as the molecular deformity of the carcinogen and the population of the diequatorial diol conformation increase (*19*); however, the detailed structural basis for this activity difference at the molecular level is not well understood.

<sup>1</sup> Abbreviations: BaP, benzo[a]pyrene; BaPDE, benzo[a]pyrene-7,8-dihydrodiol-9,10-epoxide; BaP-N<sup>2</sup>-dG, 10-(deoxyguanosin-N<sup>2</sup>-yl)-7,8,9-trihydroxy-7,8,9,10-tetrahydrobenzo[a]pyrene; BcP, benzo[c]phenanthrene; BcPDE, benzo[c]phenanthrene-3,4-dihydrodiol-1,2-epoxide; BF-N<sup>2</sup>-dG, 5a-(deoxyguanosin-N<sup>2</sup>-yl)-3,4,5-trihydroxy-3,4,5,5a-tetrahydrobenzo[ghi]fluoranthene; BF-N<sup>6</sup>-dA, 5a-(deoxyadenosine-N<sup>6</sup>-yl)-3,4,5-trihydroxy-3,4,5,5a-tetrahydrobenzo[ghi]fluoranthene; BF-N<sup>4</sup>-dC, 5a-(deoxycytosine-N<sup>4</sup>-yl)-3,4,5-trihydroxy-3,4,5,5a-tetrahydrobenzo[ghi]fluoranthene; B[ghi]FDE, benzo[ghi]fluoranthene-3,4-dihydrodiol-5,5a-epoxide; COSY, correlation spectroscopy; MALDI, matrix-assisted laser desorption ionization mass spectrometry; NOE, nuclear Overhauser effect; NOESY, nuclear Overhauser spectroscopy; PAHs, polycyclic aromatic hydrocarbons; PSD, post-source decay; syn-trans-tetraol, 3 $\beta$ ,4 $\beta$ ,5 $\beta$ ,5a $\alpha$ -tetrahydroxy-3,4,5,5a-tetrahydrobenzo[ghi]fluoranthene; syn-cis-tetraol, 3 $\beta$ ,4 $\beta$ ,5 $\beta$ ,5a $\beta$ -tetrahydroxy-3,4,5,5a-tetrahydrobenzo[ghi]fluoranthene.

\* To whom correspondence should be addressed. Phone: (401) 874-5024. Fax: (401) 874-5048. E-mail: bcho@uri.edu.

<sup>†</sup> University of Rhode Island.

<sup>‡</sup> Loyola University.

<sup>§</sup> National Center for Toxicological Research.

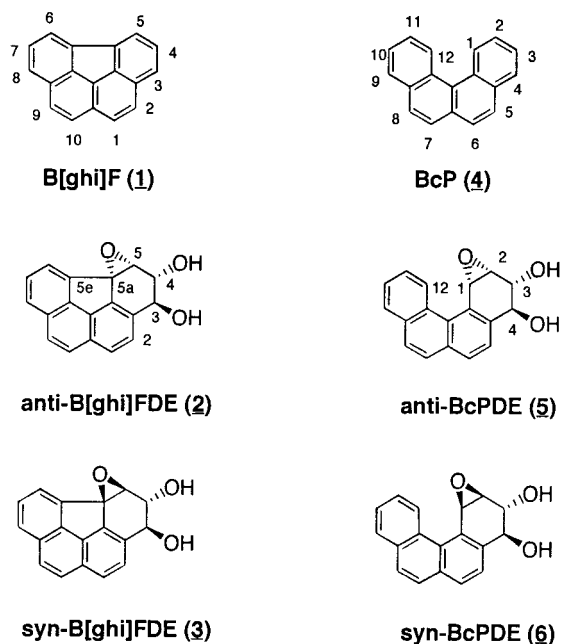


**Figure 1.** Chemical structures and numberings of (a) benzo[ghi]fluoranthene (B[ghi]F, **1**) and its diolepoxide derivatives, anti- and syn-3,4-dihydrodiol 5,5a-epoxides (B[ghi]FDE, **2** and **3**); benzo[c]phenanthrene (BcP, **4**) and its diolepoxides, anti- and syn-benzo[c]phenanthrene 3,4-dihydrodiol 1,2-epoxides (BcPDE, **5** and **6**).

An understanding of how subtle changes in the structures of diolepoxides lead to different biological outcomes requires systematic structure–function investigations. One powerful approach is to employ structure analogues whose conformational structures are well-defined. We have recently reported the synthesis of anti- and syn-benzo[ghi]fluoranthene-3,4-dihydrodiol-5,5a-epoxides (anti- and syn-B[ghi]FDE, **2** and **3**, Figure 1) as putative diolepoxide metabolites of benzo[ghi]fluoranthene (**1**) (20), a ubiquitous environmental pollutant (1, 21). These compounds are the rigid structural analogues of the extensively studied anti- and syn-benzo[c]phenanthrene-11,12-dihydrodiol-13,14-epoxide (anti- and syn-BcPDE, **5** and **6**, Figure 1), respectively (22–30). The structure of **1** is different from benzo[c]phenanthrene (**4**) in that the four benzene rings in the molecule are fused directly to the cyclopentane ring that makes up the fjord-region. Although both **1** and **4** are found to be inactive as complete carcinogens on mouse skins (22, 31), the diolepoxide metabolites of the latter (i.e., **5** and **6**) exhibit strong mutagenic/tumorigenic activities in both mammalian and bacterial systems (9, 10, 16, 22, 29, 30). While the structures of B[ghi]FDE (**2** and **3**) are virtually isomeric to BcPDE (**5** and **6**), the linkage between C5a and C5e in the fjord-region causes the molecules to be planar and the resulting rigidity causes their diol conformations to be locked into pseudo-diequatorial ( $J_{3,4} = 8.1$  Hz) and pseudo-diaxial ( $J_{3,4} = 2.1$  Hz) conformations, respectively (20). This is contrasted with the nonplanar **5** ( $J_{3,4} = 8$  Hz) and **6** ( $J_{3,4} = 9$  Hz), both of which are known to exist primarily as pseudo-diequatorial conformations (23). Therefore, **2** and **3** are regarded as conformational isomers specifically at the C3 and C4 carbons and could serve as models of **5** and **6** in diequatorial and diaxial configurations in structure–function studies. The interactions of **5** and **6** with DNA have been well-documented, i.e., the structures of all 16 possible DNA

adducts derived from the reactions between the four configurational isomers of BcPDE and purine deoxynucleosides have been fully characterized (24, 27).

In the present paper, we report spectral characterization of adducts and tetraols formed from *in vitro* reactions of **3** with calf-thymus DNA. A similar characterization of DNA adducts and tetraols derived from the corresponding anti-isomer **2** was described in the preceding paper in this issue. In addition, we have conducted comparative binding experiments involving reactions of **2**, **3**, and **5** either with native or denatured calf-thymus DNA under identical experimental conditions. The extent of DNA-adduct formation as opposed to solvolysis, the base selectivity (i.e., dA/dG ratio), and the mutagenicity data have been comparatively analyzed and the results are discussed in terms of the possible roles of molecular deformity and diol conformation in diolepoxide–DNA interactions.

## Experimental Procedures

**Chemicals. Caution:** The diolepoxides **2**, **3**, and **5** should be regarded as potential carcinogens and any skin contact should be avoided. These compounds were handled in accordance with NIH Guidelines (32).

Racemic anti- (**2**) and syn-B[ghi]FDE (**3**) were prepared as described previously (20). Racemic anti-BcPDE (**5**) was a generous gift from Dr. R. G. Harvey at the Ben May Institute for Cancer Research, University of Chicago. Poly(dG-dC)·poly(dG-dC) and poly(dA-dT)·poly(dA-dT), calf-thymus DNA, DNase I, snake venom phosphodiesterase, and alkaline monophosphatase were all purchased from Sigma (St. Louis, MO). Reagent- and HPLC-grade solvents were obtained from Fisher (Pittsburgh, PA) and used without further purification. All other chemicals were purchased from Aldrich (Milwaukee, WI).

**Instrumentation.** The instrumentation and procedures used to characterize the products of the reactions of **3** with DNA are similar to those described in the preceding paper in this issue and are briefly summarized here. HPLC analyses were conducted on a Waters Associate HPLC system equipped with model 501 pumps, a U6K injector, a 680 automated gradient controller, and a Hitachi L-3000 photodiode array detector. Specific HPLC conditions are indicated in the text and the figure legends. Combined HPLC samples were concentrated using a model AES1000-120 SpeedVac concentrator (Forma Scientific, Inc., Marietta, OH).  $^1\text{H}$  NMR spectra were recorded at ambient temperatures on a Bruker AM300 NMR spectrometer, operating at 300 MHz. Chemical shifts were expressed in parts per million with respect to TMS by assigning the tallest residual solvent peak; 2.05 and 3.31 ppm for acetone- $d_6$  and methanol- $d_4$ , respectively. COSY, NOESY, one-dimensional NOE difference and decoupling experiments were routinely conducted using standard Bruker softwares. Matrix-assisted laser desorption ionization (MALDI) mass spectra of adducts and tetraols were acquired with a R. M. Jordan, Co. (model D850) time-of-flight mass spectrometer (Grass Valley, CA). PSD product ion spectra were acquired with a PerSeptive Biosystems, Inc. Voyager DE-EP mass spectrometer (Framingham, MA) at the Washington University Resource for Biomedical and Bio-organic Mass Spectrometry in St. Louis, MO. The details of mass spectrometer operation were described previously and also in the preceding paper in this issue (33, 34). UV spectra were recorded on a Hitachi U-2000 UV–Vis spectrophotometer. CD spectral measurements in methanol were made on a Jasco model J500A spectropolarimeter (National Center for Toxicological Research, Jefferson, AR). Molecular modeling work was conducted using version 3.0 of the CAChe default MM2 force field.

**Reaction of **3** with Calf-Thymus DNA.** Reactions of **3** with calf-thymus DNA, poly(dG-dC)·poly(dG-dC), and poly(dA-dT)·poly(dA-dT) and subsequent isolation of adducts and tetraols were conducted as described for the anti-isomer **2** in the

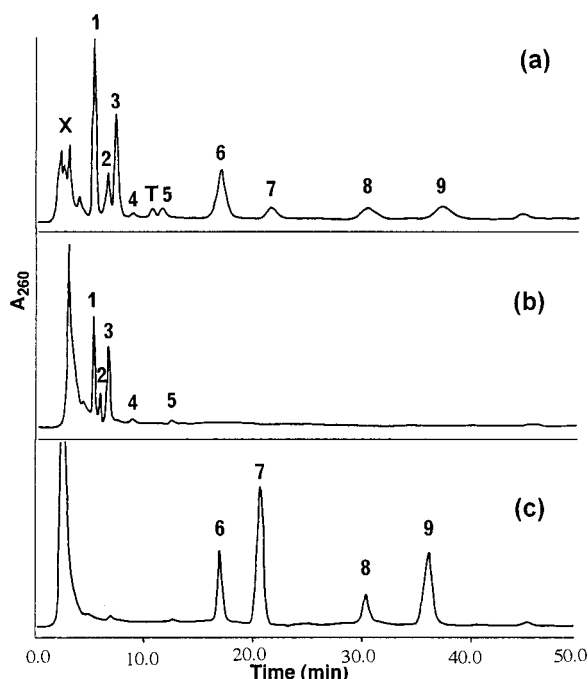


**Figure 2.** HPLC chromatograms obtained from the reaction of the racemic **3** with (a) calf-thymus DNA; (b) poly(dG·dC)poly(dG·dC); and (c) poly(dA·dT)poly(dA·dT). The adducts are numerically labeled in decreasing order of polarity: syn-trans-BF(R,S)-N<sup>2</sup>-dG (syn-1), syn-cis-BF(R)-N<sup>2</sup>-dG (syn-2), syn-cis-BF(S)-N<sup>2</sup>-dG (syn-3), syn-trans-BF(R)-N<sup>4</sup>-dC (syn-4), syn-trans-BF(S)-N<sup>4</sup>-dC (syn-5), syn-trans-BF(R)-N<sup>6</sup>-dA (syn-6), syn-trans-BF(S)-N<sup>6</sup>-dA (syn-7), syn-cis-BF(R)-N<sup>6</sup>-dA (syn-8), syn-cis-BF(S)-N<sup>6</sup>-dA (syn-9) (see Figure 3 for the structures); X: normal nucleosides; T-tetraols (Vydac ODS, 4.6 × 25 mm, 5 μm, 50% methanol/water, 1 mL/min).

preceding paper in this issue. Figure 2 shows representative chromatographic profiles for these reactions.

**Comparative DNA Binding Experiments with Native or Denatured Calf-Thymus DNA.** The three racemic di-epoxides, **2**, **3**, and **5**, were reacted separately with either native or denatured calf-thymus DNA under identical reaction conditions. Denatured DNA was prepared immediately before experiments by boiling calf-thymus DNA for 2 min. Di-epoxide solution (0.1 mL, 1 mg/mL acetone) and 1.0 mL of native (1 mg/mL)- or denatured calf-thymus DNA (1 mg/mL) were mixed in Tris-HCl buffer (0.5 mL, 50 mM, pH ~7). After incubation at 37 °C in the dark for 48 h, the DNA digestion was carried out as described in the preceding paper in this issue. The aqueous solution was treated with 26 μL of 1 M magnesium chloride, 50 μL of 1% sodium azide, and 500 kilounits of DNase I (0.28 mg) in 64 μL of 50 mM, pH ~7, Tris-HCl buffer and incubated overnight at 37 °C. This was followed by addition of 75 μL of 1 M Tris base and 0.08 units of snake venom phosphodiesterase in 64 μL of 0.2 M Tris-HCl buffer (pH 9.0). After 48 h of incubation at 37 °C, 5 units of alkaline monophosphatase was added, and the incubation continued overnight. After the usual Sep-Pak procedure, combined methanol extracts were analyzed by HPLC (Figure 2a). Relative amounts of dA and dG adducts were determined by comparing the ratios of the integrated peak areas measured at 260 nm. The organic extract from each reaction was analyzed similarly. The percentages of DNA adducts formed during the incubation was calculated by subtracting the amount of the residual di-epoxides and the tetraols. It was assumed that the extinction coefficients of tetraols at 260 nm were similar to those of the starting di-epoxides.

The overall chromatograms of fractions derived from **2** and **3** are nearly identical to those derived from the semi-prep scale procedures. The chromatographic adduct profiles derived from

**5** are consistent with those reported in the literature, except the peaks belonging to the R isomer of trans-opened dG adduct, syn-trans-5a-(deoxyguanosin-N<sup>2</sup>-yl)-3,4,5-trihydroxy-3,4,5,5a-tetrahydrobenzo[ghi]fluoranthene (syn-trans-BF(R)-N<sup>2</sup>-dG), and the S isomer of the cis-opened adenosine adduct, syn-trans-5a-(deoxyadenosin-N<sup>6</sup>-yl)-3,4,5-trihydroxy-3,4,5,5a-tetrahydrobenzo[ghi]fluoranthene (syn-cis-BF(S)-N<sup>6</sup>-dA) (24, 27). The peaks corresponding to these two compounds are unresolved in the chromatogram. It should be noted that a racemic mixture of **5** was used in this study, while Agarwal et al. reacted each enantiomers separately (27).

**Salmonella Mutagenicity Assay.** Reversions were measured in *Salmonella typhimurium* test strain TA100 (kindly provided by Dr. Bruce Ames) using the plate-incorporation assay (35). The assays included untreated control cultures as well as cultures containing various concentrations of di-epoxides dissolved in DMSO. For the parent PAH, S9 (Aroclor 1254-induced male F344 rat liver, Molecular Toxicology, Inc., Boone, NC) was employed in which 2 mL of molten top agar (with 0.5 mM histidine and biotin) was mixed with 500 μL of S9 mix, 100 μL of the test strain culture, and 50 μL of the test chemical or DMSO. The S9 mix included the following ingredients (final concentrations in the S9 mix): sodium phosphate buffer (100 mM, pH 7.4); KCl (33 mM); MgCl<sub>2</sub> (8 mM); NADP<sup>+</sup> (4 mM); glucose-6-phosphate (5 mM), and S9 in a concentration of 0.04 mL/mL of mix. Blank assays were performed by mixing the bacteria with the PAH of interest with all the substance detailed above except S9. In the black assay, KCl was substituted (in the same concentration) for S9. The mixtures were poured into plates containing Vogel-Bonner salts with 2% glucose and incubated at 37 °C for 72 h. Cultures treated with 5 or 10 μg of 2-aminofluorene or benzo[a]pyrene were included in each assay, with S9 activation, as positive controls. The assays were conducted in triplicates.

## Results

**Structure Characterization of Tetraols and DNA Adducts.** Upon completion of reaction of **3** with calf-thymus DNA, tetraols and the unreacted **3** were extracted with ether or ethyl acetate, while modified DNA adducts in the aqueous layer were subjected to a successive enzymatic digestion to deoxynucleosides. Sufficient amounts of tetraols and deoxynucleoside adducts were collected by a semipreparative reversed-phase HPLC for spectral characterization. Representative HPLC profiles from reactions with calf-thymus DNA and polynucleotides are shown in Figure 2. Figure 3 shows the full structures of deoxynucleoside adducts and tetraols derived from reaction of the racemic **3** with calf-thymus DNA. The structures of the adducts are derived from the opening of the epoxide ring of each enantiomer of **3** at C5a by the exocyclic amino groups of dG (N<sup>2</sup>), dA (N<sup>6</sup>), and dC (N<sup>4</sup>) via either trans- or cis-openings. The isolated DNA adducts are labeled as syn-1–9 according to the order of elution as shown in Figure 2; syn-trans-BF(S or R)-N<sup>2</sup>-dG (syn-1), syn-cis-BF(R)-N<sup>2</sup>-dG (syn-2), syn-cis-BF(S)-N<sup>2</sup>-dG (syn-3), syn-trans-BF(R)-N<sup>4</sup>-dC (syn-4), syn-trans-BF(S)-N<sup>4</sup>-dC (syn-5), syn-trans-BF(R)-N<sup>6</sup>-dA (syn-6), syn-trans-BF(S)-N<sup>6</sup>-dA (syn-7), syn-cis-BF(R)-N<sup>6</sup>-dA (syn-8), syn-cis-BF(S)-N<sup>6</sup>-dA (syn-9). With native calf-thymus DNA, 33% of **3** was converted into DNA adducts. The relative percentage amount of adducts is as follows, assuming their extinction coefficients are similar at 260 nm: syn-1 (33.4%), syn-2 (10.5%), syn-3 (17.3%), syn-4 (1.4%), syn-5 (3.4%), syn-6 (13.6%), syn-7 (8.0%), syn-8 (6.0%), and syn-9 (7.0%).

As detailed in the preceding paper in this issue for the anti-adducts, the structures of the syn-adducts and syn-tetraols were characterized similarly based on analyses

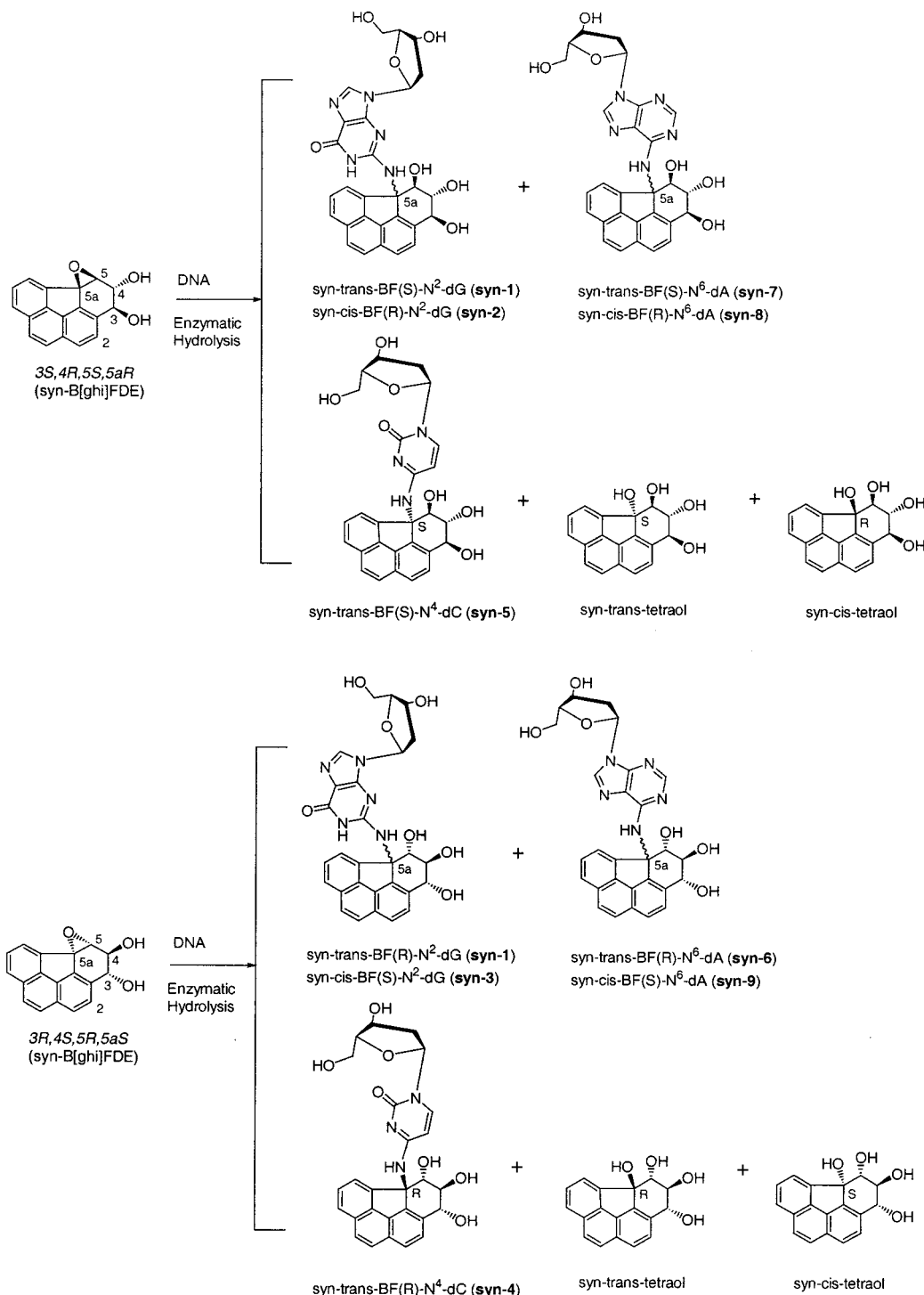


**Figure 3.** Structures of nucleoside adducts and tetraols derived from reaction of the racemic *syn*-B[ghi]FDE (**3**) with DNA. The adducts that were isolated are labeled as *syn*-1–9 according to the numbering in the HPLC profile given in Figure 2. The absolute configuration assignment (S or R) at the deoxynucleoside attachment (C5a) is specified. *syn* refers to a relative epoxide/benzylic hydroxyl configuration of **3**, i.e., the epoxide oxygen is on the same side of the molecule relative to the benzylic hydroxyl group. *trans* and *cis* refer to the reaction pattern of epoxide ring opening, where it occurs from the opposite or same side, respectively.

of <sup>1</sup>H NMR (Table 1), MALDI-MS (Table 2), UV (Figure 4) and CD (Figure 5) spectral data. PSD-MALDI spectra of (M + H)<sup>+</sup> ions of deoxynucleoside adducts revealed fragmentation patterns that are consistent with the assigned structures (Table 2) but did not permit differentiation of diastereomer adducts formed from the *trans*- or *cis*-opening of an epoxide. Diastereomeric relationships at the C5a carbon were determined by comparing the CD spectra of the HPLC fractions. The CD spectra shown in Figure 5 suggests that the four sets of diastere-

omers were separated by HPLC. Similar to the *anti*-adducts, the UV spectra of the same deoxynucleoside adducts derived from **3** are essentially identical so long as the epoxide ring opening pattern (i.e., *trans*- or *cis*-) is the same, regardless of the *anti*- and *syn*-nature of the starting diepoxide (Figure 4) (27). The absorption maximum of *cis*-adducts and *cis*-tetraol is slightly shifted (about 1–2 nm) to the shorter wavelength relative to the *trans* adducts. The epoxide ring opening pattern, i.e., *trans*- and *cis*-, was established by analyses of the

Table 1.  $^1\text{H}$  NMR Data for Adducts and Tetraols Derived from syn-B[ghi]FDE (3)<sup>a</sup>

compd	N-H	methine hydrogens (ppm)				aromatic protons
		H <sub>3</sub>	H <sub>4</sub>	H <sub>5</sub>	$J_{3,4}, J_{4,5}$	
syn-B[ghi]FDE (3)		4.83	4.75	4.68	2.1, 2.0 ( $J_{3,5} = 1.3$ Hz)	7.61 (H <sub>2</sub> , $J_{1,2} = 8.1$ Hz), 7.62-7.65 (H <sub>6,8</sub> ), 7.88 (H <sub>9,10</sub> ), 7.93 (H <sub>7</sub> , $J = 5.5, 3.1$ Hz)
syn-trans-tetraol		5.21	4.06	4.80	3.6, 2.7	7.80 (H <sub>1</sub> , $J_{1,2} = 8.2$ Hz), 7.79 (H <sub>8</sub> , $J_{7,8} = 7.9$ Hz), 7.78 (H <sub>9,10</sub> ), 7.68 (H <sub>6</sub> , $J_{6,7} = 7.1$ Hz), 7.67 (H <sub>2</sub> , $J_{1,2} = 8.2$ Hz, $J_{2,3} = 0.4$ Hz)
syn-cis-tetraol		4.58	4.71	3.50	6.4, 9.2	7.92 (H <sub>1</sub> , $J_{1,2} = 8.3$ Hz), 7.81 (H <sub>8</sub> , $J_{7,8} = 8.0$ Hz), 7.76 (H <sub>6</sub> , $J_{6,7} = 7.1$ Hz), 7.54 (H <sub>7</sub> ), 7.47 (H <sub>9,10</sub> )
syn-trans-BF(R,S)-N <sup>2</sup> -dG (syn-1) <sup>b</sup>	7.2 (bs)	~5.2	3.83	~5.2	NA	8.04 (H <sub>6</sub> ), 7.97 (H <sub>6</sub> ), 7.69 (H <sub>2</sub> ), 7.51 (H <sub>7</sub> ), 7.93-7.73 (H <sub>1,8,9,10</sub> , Gua-H <sub>8</sub> )
syn-trans-BF(S)-N <sup>4</sup> -dC (syn-5)	7.23 (bs)	5.26	3.48	5.56	7.8, 3.7	8.51 (H <sub>6</sub> , $J_{6,7} = 6.6$ Hz), 7.86 (H <sub>1</sub> , $J_{1,2} = 8.1$ Hz), 7.69 (H <sub>2</sub> , $J_{1,2} = 8.3$ Hz), 7.72-7.82 (H <sub>8,9,10</sub> ), 7.50 (H <sub>7</sub> ), 5.88 (Cyt-H <sub>5</sub> , $J_{5,6} = 7.4$ Hz), 7.95 (Cyt-H <sub>6</sub> )
syn-trans-BF(R)-N <sup>6</sup> -dA (syn-6)	7.41 (bs)	5.40	3.83	5.53	5.5, 1.5	8.14 (H <sub>6</sub> , $J_{6,7} = 7.1$ Hz), 7.68-7.88 (H <sub>1,2,8,9,10</sub> ), 7.47 (H <sub>7</sub> ), 8.24 (Ade-H <sub>2</sub> ), 8.10 (Ade-H <sub>8</sub> )
syn-trans-BF(S)-N <sup>6</sup> -dA (syn-7)	7.40 (bs)	5.39	3.83	5.53	5.4, 1.4	8.14 (H <sub>6</sub> , $J_{6,7} = 7.1$ Hz), 7.68-7.89 (H <sub>1,2,8,9,10</sub> ), 7.48 (H <sub>7</sub> ), 8.24 (Ade-H <sub>2</sub> ), 8.11 (Ade-H <sub>8</sub> )
syn-cis-BF(R)-N <sup>6</sup> -dA (syn-8)	7.42 (bs)	4.69	4.66	NA	NA	8.03 (H <sub>6</sub> , $J_{6,7} = 7.4$ Hz), 7.91 (H <sub>1</sub> , $J_{1,2} = 8.1$ Hz), 7.79-7.87 (H <sub>8,9,10</sub> ), 7.78 (H <sub>8</sub> , $J_{7,8} = 8.3$ Hz), 7.65 (H <sub>2</sub> , $J_{1,2} = 8.5$ Hz), 7.47 (H <sub>7</sub> ), 8.28 (Ade-H <sub>2</sub> ), 8.22 (Ade-H <sub>8</sub> ) <sup>c</sup>
syn-cis-BF(S)-N <sup>6</sup> -dA (syn-9)	7.41 (bs)	4.69	4.66	NA	NA	8.03 (H <sub>6</sub> , $J_{6,7} = 7.0$ Hz), 7.91 (H <sub>1</sub> , $J_{1,2} = 8.5$ Hz), 7.77-7.87 (H <sub>8,9,10</sub> ), 7.78 (H <sub>8</sub> , $J_{7,8} = 8.3$ Hz), 7.66 (H <sub>2</sub> , $J_{1,2} = 8.5$ Hz), 7.47 (H <sub>7</sub> ), 8.25 (Ade-H <sub>2</sub> ), 8.23 (Ade-H <sub>8</sub> ) <sup>c</sup>

<sup>a</sup> Spectra were measured in acetone- $d_6$  with D<sub>2</sub>O except where indicated. Chemical shifts are reported in  $\delta$  (ppm) and coupling constants are given in hertz (Hz). Abbreviation: bs, broad singlet, ND, not detectable, NA, not assigned. The spectral data for syn-2, -3, and -4 were not included due to low signal-to-noise ratio. <sup>b</sup> Taken in methanol- $d_6$ . <sup>c</sup> Chemical shifts of the adenosine H2 and H8 are sensitive to the addition of D<sub>2</sub>O. See Figures 1 and 3 for full structures.

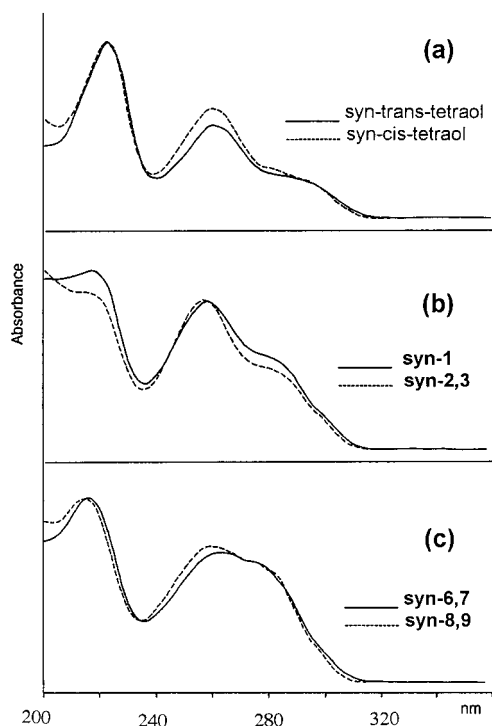


**Figure 4.** Normalized on-line UV spectra of (a) tetraols, (b) syn-BF-N<sup>2</sup>-dG, and (c) syn-BF-N<sup>6</sup>-dA adducts derived by trans (—) and cis (---) opening of **3**. Spectra of the diastereomeric pairs (i.e., syn-2 and -3, -4 and -5, -6 and -7, and -8 and -9) at the site of nucleoside attachment (C5a) are essentially identical.

chemical shift of H<sub>5</sub> and the  $J_{3,4}$  and  $J_{4,5}$  coupling constants. The pseudoaxial H<sub>5</sub> in the cis-adducts is placed directly under the shielding cone of the aromatic ring system, while the pseudoequatorial H<sub>5</sub> proton in trans-adducts protrudes away from the aromatic ring system. As in the case of anti-adducts, the absolute configuration at C5a was tentatively assigned on the basis of the empirical CD rules of traditional bay-region diolepoxides (19). The site of an epoxide opening was

similarly determined to be at C5a on the basis of several lines of evidence that includes a significant deshielding of H<sub>5</sub> compared to the corresponding tetraol precursor; a sharp exchangeable N-H proton; a small change of  $J_{4,5}$  and a large deshielding going from diolepoxide to adducts; and NOE effects on H<sub>6</sub>, H<sub>4</sub>, and the adenine H<sub>2</sub> upon irradiation of H<sub>5</sub> (see preceding paper).

**Tetraols.** The organic phase afforded a 3:2 ratio of syn-trans-tetraol ( $t_R = 6.2$  min) and syn-cis-tetraol ( $t_R = 11.8$  min) in addition to the unreacted diolepoxide at 21.7 min (Beckman Ultrasphere ODS, 4.6 mm  $\times$  25 cm, 5  $\mu$ m, 50% methanol, 1 mL/min). The  $^1\text{H}$  NMR spectra in acetone- $d_6$  showed well-resolved methine and aromatic protons, all of which have been unambiguously assigned by the general  $^1\text{H}$  NMR strategy detailed in the preceding paper (see above). The late eluting fraction at 11.8 min shows a relatively shielded H<sub>5</sub> at 3.50 ppm, which is evidence for the cis-opening. Molecular modeling indicated that the H<sub>4</sub>-C<sub>4</sub>-C<sub>5</sub>-H<sub>5</sub> dihedral angle for syn-cis-tetraol is almost antiparallel, and H<sub>5</sub> is forced into the pseudo-diaxial orientation. This is consistent with a large  $J_{4,5}$  coupling constant (9.2 Hz) observed for syn-cis-tetraol. The chemical shift and coupling characteristics of the major tetraol at 6.2 min have changed very little from the starting diolepoxide **3**, suggesting the trans-opened structure. The observed small  $J_{4,5}$  coupling constant (2.7 Hz) is consistent with the calculated H<sub>4</sub>-C<sub>4</sub>-C<sub>5</sub>-H<sub>5</sub> dihedral angle, which is somewhat less than 90°. The MALDI mass spectra of tetraols gave the (M + Li)<sup>+</sup> ions at  $m/z$  301 as the base peak, which confirms their structures. The stereochemistry of the tetraols was confirmed by MALDI-PSD product ion analysis (34). The relative stereochemistry of hydroxyl groups at C<sub>3-4-5-5a</sub> of syn-trans-tetraol and syn-cis-tetraol are trans-trans-trans and trans-trans-cis, respectively. Accordingly, the (M + Li)<sup>+</sup> ion at  $m/z$  301 of syn-trans-tetraol undergoes consecutive water losses via a 1,2-elimination to form product ions at  $m/z$  283 and  $m/z$  265 in equal intensities, while syn-cis-tetraol loses only one water molecule to

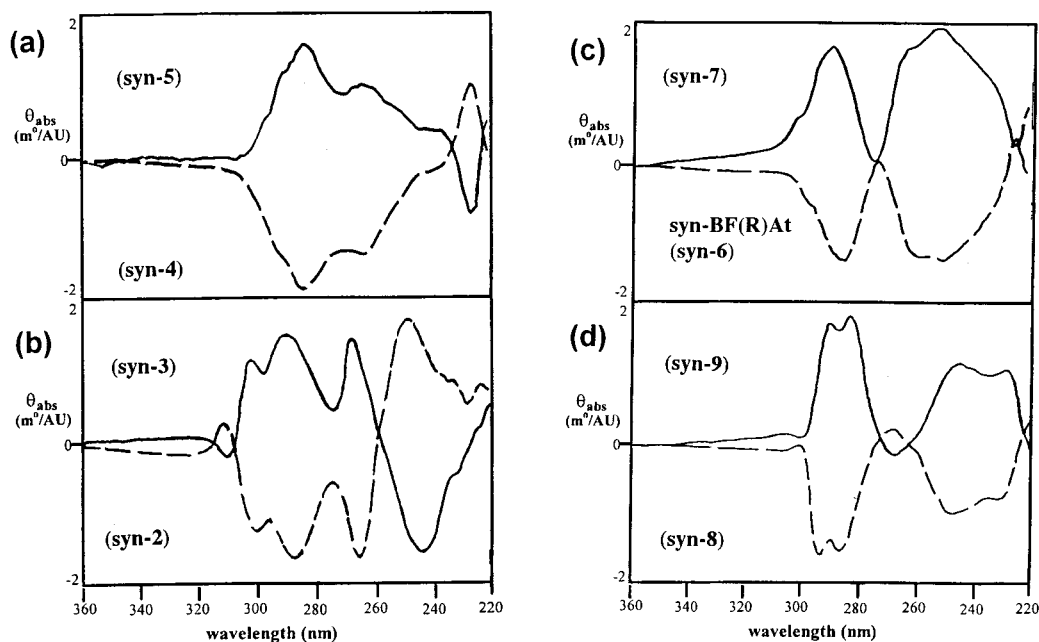


**Figure 5.** CD spectra of the adducts derived from *trans*- and *cis*-opening at C5a by the exocyclic amino groups of (a) *syn*-*trans*-BF-N<sup>4</sup>-dC (*syn*-4 and -5), (b) *syn*-*cis*-BF-N<sup>2</sup>-dG (*syn*-2 and -3), (c) *syn*-*trans*-BF-N<sup>6</sup>-dA (*syn*-6 and -7), and (d) *syn*-*cis*-BF-N<sup>6</sup>-dA (*syn*-8 and -9). The spectra were taken in pure methanol and are labeled according to the numbering in Figure 2. See Figure 3 for the chemical structures.

**Table 2.** Time-of-Flight MALDI Mass Spectra Data for Adducts and Tetraols Derived from *syn*-B[ghi]FDE (**3**)

compd	mass ions			
	[M - dR] <sup>+</sup>	[M + H] <sup>+</sup>	[M + Li] <sup>+</sup>	[M + Na] <sup>+</sup>
<i>syn</i> - <i>trans</i> -tetraol			301 (100)	
<i>syn</i> - <i>cis</i> -tetraol			301 (100)	
<i>syn</i> - <i>trans</i> -BF(RS)-N <sup>2</sup> -dG ( <b>syn</b> -1)	428 (100)	544 (40)		566 (40)
<i>syn</i> - <i>trans</i> -BF(R)-N <sup>2</sup> -dG ( <b>syn</b> -2)	428 (100)	544 (40)		566 (40)
<i>syn</i> - <i>trans</i> -BF(S)-N <sup>2</sup> -dG ( <b>syn</b> -3)	428 (100)	544 (30)		566 (55)
<i>syn</i> - <i>trans</i> -BF(R)-N <sup>4</sup> -dC ( <b>syn</b> -4)	388 (100)	504 (55)		526 (100)
<i>syn</i> - <i>trans</i> -BF(S)-N <sup>4</sup> -dC ( <b>syn</b> -5)	388 (100)	504 (35)		526 (100)
<i>syn</i> - <i>trans</i> -BF(R)-N <sup>6</sup> -dA ( <b>syn</b> -6)	412 (80)	528 (100)		
<i>syn</i> - <i>trans</i> -BF(S)-N <sup>6</sup> -dA ( <b>syn</b> -7)	412 (80)	528 (100)		
<i>syn</i> - <i>cis</i> -BF(R)-N <sup>6</sup> -dA ( <b>syn</b> -8)	412 (90)	528 (100)		
<i>syn</i> - <i>cis</i> -BF(S)-N <sup>6</sup> -dA ( <b>syn</b> -9)	412 (90)	528 (100)		

yield predominantly a single fragmentation at  $m/z$  283. A detailed account of the PSD-analyses of tetraols derived from **2** and **3** has been reported (34).

**Deoxynucleoside Adducts.** The HPLC chromatogram in Figure 2a shows at least nine adducts, which are labeled as *syn*-1–9 according to the order of decreasing polarity. Separate reactions of **3** with poly(dG-dC)·poly(dG-dC) and poly(dA-dT)·(dA-dT) were conducted, and the results were shown in Figure 2. Comparison of the results indicated clearly that the polar adducts *syn*-1,2,3,4,5 are derived from dG (or dC), while the less polar adducts *syn*-6,7,8,9 originated from dA (or dT). As shown in Figure 5, the CD spectra of *syn*-2 and -3, *syn*-4 and -5, *syn*-6 and -7, and *syn*-8 and -9 were found to be mirror images, confirming their diastereomeric relationships at the site of the deoxynucleoside attachment, C5a.

*syn*-*trans*-BF(R)-N<sup>6</sup>-dA (*syn*-6); *syn*-*trans*-BF(S)-N<sup>6</sup>-dA (*syn*-7). The MALDI mass spectra of *syn*-6 and -7 are essentially identical and showed a (M + H)<sup>+</sup> peak at  $m/z$  528 and a (M + H - dR)<sup>+</sup> fragmentation ion at  $m/z$  412, which is evidence for the presence of the B[ghi]F-dA adduct. Their CD spectra are mirror images of one another, indicating their diastereomeric relationship at C5a (Figure 5). The <sup>1</sup>H NMR spectra (not shown) of these two adducts are virtually identical and resemble those

of the dA diastereomers *anti*-4 and -5 derived from **2** described in the preceding paper. The appearance of a sharp singlet for the exchangeable N–H proton at 7.41 ppm is consistent with the deoxynucleoside attachment at C5a. A majority of signals including the benzo[ghi]fluoranthene H3,4,5-carbinolic proton network were assigned by analyses of the NOE and decoupling data, and the results are summarized in Table 1. A deshielding of H5 relative to the diepoxide precursor indicates that the pseudoequatorial H5 is forced out of the shielding zone of the aromatic ring system. The observed coupling constants ( $J_{3,4} = 5.6$  Hz,  $J_{4,5} = 1.4$  Hz) are largely consistent with the calculated dihedral angles for a *syn*-*trans*-dA adduct ( $\angle$ H4–C4–C5–H5 = 70° and  $\angle$ H3–C3–C4–H4 = 133°). On the basis of these data, *syn*-6 and -7 were assigned to the adducts derived from the *trans*-opening of the epoxide at C5a by the amino group of dA. Additional evidence for the *trans*-dA adduct structure is that the UV (Figure 4) and CD (Figure 5) spectral features of *syn*-6 and -7 closely resemble those of the *trans*-opening dA adducts (*anti*-4 and 5) derived from the *anti* diepoxide **2**. The absolute configurations at C5a of adduct-6 and -7 were tentatively assigned as R and S, respectively, on the basis of their CD shape at 280 nm.

**Table 3. Percent Adduct Formation (%) and dA/dG Ratio in Reactions of anti- (2) and syn-B[ghi]FDE (3) and anti-BcPDE (5) with Native and Denatured Calf-Thymus DNA<sup>a</sup>**

calf-thymus DNA	anti-B[ghi]FDE (2)		syn-B[ghi]FDE (3)		anti-BcPDE (5)	
	native	denatured	native	denatured	native	denatured
% adduct formation	57	47	33	16	71	64
dA/dG ratio	0.79	0.42	0.56	0.23	1.41	0.54

<sup>a</sup> Quantification is based on UV absorption measurements, assuming the extinction coefficients for all adducts are similar at 260 nm. See Experimental Procedures for details.

*syn-cis-BF(R)-N<sup>6</sup>-dA (syn-8); syn-cis-BF(S)-N<sup>6</sup>-dA (syn-9)*. The two most hydrophobic adducts, syn-8 and -9, showed virtually identical <sup>1</sup>H NMR, UV, and MALDI mass spectral patterns, with the exception of their mirrored CD images (Figure 5d). The mass spectra are essentially identical to those of the syn-6 and -7 adducts described above. Thus, syn-8 and -9 were assigned as the diastereomeric dA adduct pair arising from the cis opening at C5a (Figure 3). The majority of signals in the <sup>1</sup>H NMR spectrum of syn-8 recorded in acetone-*d*<sub>6</sub> have been assigned by the usual analyses of decoupling, NOE and COSY experiments and are consistent with the assigned structure (Table 1). It was observed that the adenine H2 signal overlapped with the adenine H8 signal at 8.2 ppm, but moved downfield by 0.08 ppm upon the addition of D<sub>2</sub>O (H2:8.28 ppm; H8:8.22 ppm). The H5 signal could not be definitely assigned due to solvent interference. This solvent interference and the overlapping of the H3 and H4 protons did not allow measurement of the *J*<sub>3,4</sub> and *J*<sub>4,5</sub> coupling constants. The UV spectra of the syn-8 and -9 pair are identical and very similar to those of the cis-opened dA adducts derived from **2** (preceding paper). The absorption maxima at 260 nm was shifted slightly to shorter wavelength relative to the trans-opened dA pair (syn-6 and -7). A similar hypsochromic shift was observed for the cis-opened dA derived from **2**. According to CD shape (Figure 5), syn-8 and -9 were assigned to the R and S isomers, respectively.

*syn-trans-BF(R)-N<sup>4</sup>-dC (syn-4); syn-trans-BF(S)-N<sup>4</sup>-dC (syn-5)*. The MALDI mass spectra of syn-4 and -5 are nearly identical and consistent with what is expected for a dC adduct. The predominant sample specific ions observed are the (M + Na)<sup>+</sup> at *m/z* 526 and the (M + H - dR)<sup>+</sup> at *m/z* 388. Their relative intensities are summarized in Table 2. The <sup>1</sup>H NMR spectrum of syn-5 recorded in acetone-*d*<sub>6</sub> is also similar to anti-3 and reveals a typical cytosine H5-H6 coupling (*J*<sub>5,6</sub> = 7.4 Hz). The observed coupling constants (*J*<sub>3,4</sub> = 7.8 Hz and *J*<sub>4,5</sub> = 3.7 Hz) and the deshielded chemical shift of H5 support a dC adduct structure formed by a trans-opened diol-epoxide at the C5a carbon. The <sup>1</sup>H NMR spectrum of syn-4 was found to be almost identical to that of syn-5. The UV spectra of the two diastereomeric dC adduct pairs are essentially identical to each other and the overall pattern is very similar to that of the dC adduct (anti-3) obtained from **2** (preceding paper). The CD spectrum of syn-4 also resembles closely that of anti-3, which was assigned to R, and is a mirror image of syn-5. Thus, syn-4 and -5 were tentatively assigned to the R and S isomers of cis-opened dC adducts, respectively.

*syn-trans-BF(R,S)-N<sup>2</sup>-dG (syn-1)*. The MALDI spectrum of this polar fraction gave ions consistent with that of a dG adduct. The three most prominent peaks are at *m/z* 566, *m/z* 544, and *m/z* 428 corresponding to the (M + Na)<sup>+</sup> ion, and (M + H-dR)<sup>+</sup> ion, respectively (Table 2). The UV and mass spectra are similar to those of the dG

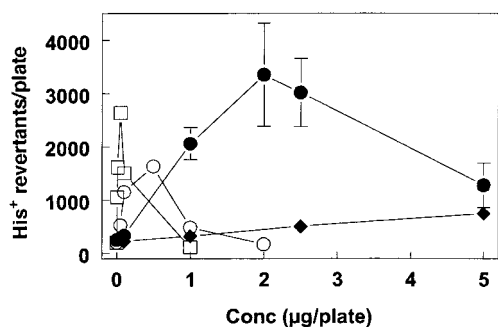
adduct (anti-1) derived from **2**. However, the <sup>1</sup>H spectrum of syn-1 revealed H6 as two doublets at 8.04 and 7.97 ppm in an equal intensity (not shown). Similarly, H7 appeared as two apparent triplets at around 7.5 ppm. The anomeric H1' sugar proton, which appeared as a multiplet at 5.47 ppm, became separated in methanol-*d*<sub>4</sub> into two clean doublet of doublets in an equal ratio. The CD spectra of syn-1 is similar to that of anti-1 (preceding paper), but its features are not clearly defined. Taken all together, it was concluded that this fraction is a mixture of two dG adducts, presumably diastereomeric at C5a.

*syn-cis-BF(R)-N<sup>2</sup>-dG (syn-2); syn-cis-BF(S)-N<sup>2</sup>-dG (syn-3)*. The MALDI mass spectra of syn-2 and -3 show the same ion formation characteristics as syn-1 (Table 2), but the CD spectra of these compounds are mirror images of each other. The <sup>1</sup>H NMR spectra of the two adducts are very similar. Since syn-1 was assigned to a diastereomeric mixture of trans-dG adducts, syn-2 and -3 were tentatively assigned as the isomeric pair of cis-opened dG-adducts. On the basis of the CD shapes, syn-2 and -3 were assigned as the R and S diastereomer, respectively.

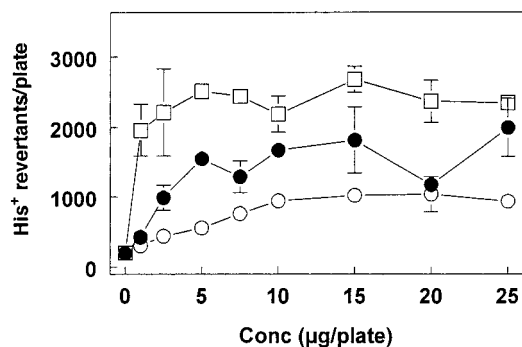
**Comparative DNA Binding Studies.** Table 3 summarizes the percentages of the three diolepoxides, **2**, **3**, and **5**, trapped by either native or denatured calf-thymus DNA. The extent to which a diolepoxide reacts with DNA is provided in terms of the fraction of the diolepoxide trapped as DNA adducts under given conditions. The deoxynucleoside adducts as well as tetraols derived from **3** are characterized in the present study. Similar work with **2** was conducted in the preceding paper. All 16 possible purine deoxynucleoside adducts derived from **5** and **6** have been characterized previously (24, 27). Therefore, HPLC conditions for their separation and quantification are well-known and were used in the present study. With native calf-thymus DNA, 57% of **2** was converted into DNA adducts, whereas much less (33%) conversion took place for the corresponding syn isomer **3**. A 71% conversion was observed for **5**, which is in good agreement with the range of values reported previously (60–75%) (39, 42). The percentage of **5** trapped in DNA is the highest among the three diolepoxides investigated.

Table 3 also lists the dA/dG ratios derived from the three diolepoxides with native or denatured calf-thymus DNA. The anti-diolepoxide **2** showed a greater affinity toward dA over dG (0.79) as compared to the syn-isomer **3** (0.56) when reacted with native DNA. The dA/dG ratio was found to be significantly higher with **5** (1.41). Going from native to denatured DNA, the extent of adduct formation with dA is diminished, while the adduction with dG is enhanced. With denatured DNA, however, the dA/dG ratio (0.54) of **5** is comparable to that (0.42) of **2**.

**Mutagenicity Testing.** Mutagenic activities of **2**, **3**, and **5** were measured and compared using a *Salmonella typhimurium* TA100 strain and the protocol of Glatt et



**Figure 6.** Ames mutagenicity data for anti-B[ghi]FDE **2** (●), syn-B[ghi]FDE **3** (◆), anti-BcPDE **5** (○), and anti-BaPDE (□). Each point represents the mean  $\pm$ SD of triplicate plates. To enhance clarity, error bars were removed from doses of  $\leq 0.05$   $\mu$ g/plate.



**Figure 7.** Ames mutagenicity data for the parent PAHs, benzo[ghi]fluoranthene **1** (●), benzo[c]phenanthrene **4** (○), and benzo[a]pyrene (□) in the presence of S9-mix. Each point represents the mean  $\pm$ SD of triplicate plates.

al. (9) (Figure 6). This strain has been used extensively with other diolepoxides (9). Anti-BaPDE was used as a reference diolepoxide. The specific mutagenicities observed for anti-BaPDE and **5** are comparable to the values reported in the literature (9). The planar diolepoxides, **2** and **3**, were found to be substantially less potent than the reference compounds. For example, **2** is about six times less potent than **5**, but is seven times more potent than the syn-isomer **3**. The mutagenicities of the parent compounds, B[ghi]F, BcP, and BaP were also measured in the presence of the S9-mix activation system (Figure 7). As expected, BaP was the most mutagenic, but B[ghi]F was found to be consistently more mutagenic than BcP over a wide range of concentration ( $\sim 25$   $\mu$ g/plate).

## Discussion

The aim of the work described here was 3-fold. One, we isolated and characterized the adducts and tetraols formed during the *in vitro* reactions of **3** with calf-thymus DNA. The second goal was to carry out comparative binding studies of compounds **2**, **3**, and **5** with calf-thymus DNA. The third aim was to compare the mutagenicity of these three compounds. These studies were designed for the purpose of gaining insight into the reactivity and mutagenicity of different diolepoxide conformations toward DNA. In the preceding paper in this issue, we described spectral characterization of the structures of seven DNA adducts and two anti-tetraols derived from **2**. The *in vitro* DNA reaction with the syn-isomer **3** in the present study provided a total of nine DNA adducts and two syn-tetraols, which have been

similarly characterized by analyses of PSD-MALDI-MS,  $^1\text{H}$  NMR, UV, and CD spectral data. As in the case of **2**, the major deoxynucleoside adducts from **3** are also those derived from the reactions on the exocyclic amino groups of dA and dG (Figure 3). A complete set of dA adducts was obtained as a result of the trans- (syn-6 and -7) or cis- (syn-8 and -9) openings of the epoxide at the dibenzylic site, C5a. Unlike the anti-isomer (preceding paper), the reaction of the syn-isomer with calf-thymus DNA did not yield a measurable amount of N<sup>7</sup>-guanine adduct. A diastereomeric pair of trans-dC adducts (syn-4 and -5) was isolated. Formation of dC-adducts from other PAH diolepoxides has been well-documented in the literature (36, 37). The absolute configurations at the site of deoxynucleoside attachment (i.e., C5a) were assigned tentatively on the basis of the empirical CD rules that have been established for bay-region diolepoxides (19). The solvolysis of **2** gave the trans-tetraol predominantly (>95%) (preceding paper); however, in the present study the solvolysis of **3** provided a 60:40 mixture of trans- and cis-tetraols, respectively. This observation is consistent with the suggestion that the structurally similar syn-fluoranthene-2,3-dihydrodiol-1,10b-epoxide undergoes solvolysis exclusively by a SN1 mechanism. The ring opening of the diolepoxide is facilitated through the anchimeric assistance of the hydroxyl group attached to the benzylic carbon (38).

Comparative DNA-binding experiments involving **2**, **3**, and **5** were conducted in order to gain insight into the structural basis of molecular deformity and diol conformation in the mechanism of diolepoxide-DNA interaction. An obvious concern here is a simple assumption that the structure of **2** is identical with the nonplanar **5** in all aspects, except for the deformity of the aromatic ring system and the rigid diol conformation (Figure 1). We have shown that both **2** (preceding paper) and **3** (this paper) indeed behave like BcPDE and other traditional diolepoxides, allowing the epoxide ring opening to occur in the expected manner at the sterically hindered dibenzylic site, C5a. Nonetheless, it is possible that the additional carbon-carbon bridge in the fjord region of **2** and **3** could change chemical reactivity, base selectivity, and regio-chemistry of the epoxide in such a way that would complicate interpretations. Other factors that could contribute to changes in selectivity include possible unforeseen inter-related steric effects and the difference in the electronic effects of hydroxyls being pseudo-diaxial as opposed to having a pseudo-diequatorial conformation. Despite these uncertainties, the comparative DNA binding and mutagenicity experiments involving **2**, **3**, and **5** have yielded some potentially interesting results.

The binding studies using native calf-thymus DNA revealed that 57% of **2** was converted into DNA adducts, whereas much less (33%) conversion was obtained for the corresponding cis-isomer **3** (Table 3). This is contrasted with a 71% conversion observed for **5**. These findings are consistent with previous findings that the epoxide ionization is favored by the presence of a larger number of planar aromatic rings, thereby facilitating solvolysis over DNA adduct formation (19, 39). For example, it has been shown that hydrolysis of the diolepoxides of the five-ring benzo[c]chrysene is about 5-fold faster than the corresponding four-ring benzo[c]phenanthrene derivatives (40, 41). Similarly, the gain of planarity in **2** and **3** would stabilize the presumed cation at C5a, thus favoring solvolysis over DNA adduct formation. The steric crowd-

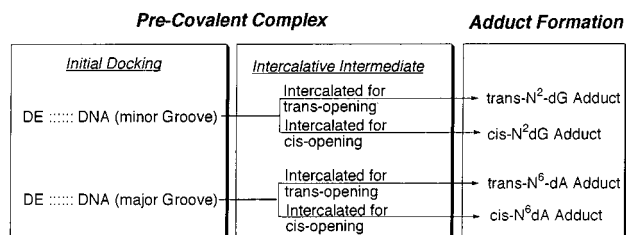


**Figure 8.** A schematic representation of the two-stage diolepoxi-DNA interaction.

ing in the fjord-region diolepoxi **5**, however, would lead to distortion from planarity, which hinders charge delocalization, thereby allowing it to preferentially react with DNA. Lewis-Bevan et al. have suggested an alternative possibility that the electrostatic stabilizing interaction between the epoxide oxygen and H12 in the fjord region of the in-conformations may be responsible for its favorable interaction with DNA (43). The reason for the difference in the extent of adduct formation between **2** and **3** is not immediately clear, but it seems unlikely to be the result of pure electronic factors since the two molecules are geometric isomers, differing only in their diol conformations (i.e., pseudo-diequatorial and pseudo-diaxial diol conformations, respectively). Likewise, the electronic argument does not explain why **3** exhibits a substantially lower dA/dG ratio (0.56) than the corresponding anti-isomer **2** (0.79). It is clear, however, that the base selectivity may be attributed to the differences in their diol configurations. It has been shown that DNA structure has significant influence on adduct distribution (17, 18, 42). For the three cases investigated, the amount of diolepoxi trapped by denatured calf-thymus DNA was generally lower as compared with native calf-thymus DNA, with the effect most significant for **3** (49% reduction). The results are summarized in Table 3. A similar trend was observed for base selectivity; the extent of adduct formation with dA is diminished, while the adduction with dG is enhanced, going from native to denatured DNA. Upon reaction with denatured DNA, the dA/dG ratio (0.54) of **5** is similar to that (0.42) observed for the planar analogue **2**, indicating that the planarity of the aromatic ring system does not matter much in the absence of the helical structure of DNA. These data indicate the importance of the secondary helical structure of DNA for both DNA binding and base selectivity.

Steric factors have been shown to influence base selectivity in the pre-interaction of diolepoxi and DNA (19). The exocyclic amino group of dG resides in the minor groove (vertical entrance width 5.7 Å) of a B-DNA, whereas that of dA is located in the major groove (width 11.7 Å) (44). The planar diolepoxi **2** and **3** would fit well in the narrow minor groove, while the nonplanarity of **5** limits its access to the minor groove. In general, diolepoxi-DNA interaction can be explained by a two-stage model ("Pre-Covalent Complex" and "Adduct Formation") depicted in Figure 8. Two possibilities exist at the initial docking stage for noncovalent association of a diolepoxi, either with the minor (for dG adducts) or major groove (for dA adducts) of DNA. Base selectivity is, therefore, determined at an early initial docking stage. Each of these complexes is then proceeded by at least two intercalative intermediates, one giving rise to a trans-opening and one giving rise to a cis-opening. The structural basis of epoxide opening is not well understood, but the directional preference of epoxide opening (i.e., cis-

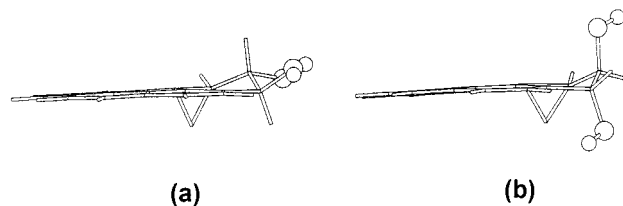


**Figure 9.** Energy-minimized structures of (a) **2** and (b) **3**. Diol functional groups are highlighted with small circles.

vs trans-) is known to be controlled by both the epoxide and diol conformations and is closely related to how a diolepoxi interacts with the secondary structure of DNA (19). Cosman et al. have shown that the BcP residues in complementary 11-mer DNA duplexes containing enantiomeric 1(R)-(+)- or 1(S)-(-)-trans-anti-BcP-N<sup>6</sup>-dA lesions are intercalated into B-type DNA with insertion pointing to the 5'- and 3'-sides of the modified dA residues, respectively (45, 46). In both cases, the modified dA residues retain regular Watson-Crick base pairings with local unwinding and stretching of the helix to accommodate the intercalated aromatic moiety. A similar conformation was obtained with the related (+)-trans-anti-benzo[g]chrysene-N<sup>6</sup>-dA adduct in the identical base sequence context (47). These structures may resemble the intercalative intermediate for dA adducts, except that there is no covalent linkage between the benzylic carbon and dA. Studies involving complete sets of BaP-N<sup>2</sup>-dG adducts have also been done and the resulting structures could serve as models for the intercalative intermediate of dG adducts. The two enantiomeric cis-anti-BaP-N<sup>2</sup>-dG adducts assume base-displaced intercalative conformations, while the two trans-adducts are characterized by minor groove conformations (3). Earlier studies of reactions of dihydrodiol S,R-epoxides with DNA indicate that trans-opening precedes binding to dA; however, bonding to dG is generally switched from trans- to cis- on inverting the diol configuration from diaxial to diequatorial (19). This means that the diol and epoxide functions are more important determinants for the directional preference of the dG reaction (in the minor groove) than for those leading to the dA reaction (in the major groove). The final adduction step involves an eventual covalent bonding between the epoxide ring and the exocyclic amino groups of each deoxynucleoside (Figure 8).

Energy minimization studies show that the overall surface structure of **2** is essentially flat throughout the entire molecule, whereas **3** is T-shaped due to the pseudo-diaxial diol conformation (Figure 9). As discussed earlier, the base selectivity is determined at an initial docking pre-covalent complex stage. Both **2** and **3** would fit into the minor groove assuming that the aromatic ring portion makes initial contact to DNA for eventual intercalation. Preliminary docking experiments using B-DNA as a receptor have revealed a possibility of forming hydrogen bondings between the T-shaped diols of **3** (Figure 9b) and the nearby negatively charged phosphate backbone of DNA. This is not the case for the anti-isomer **2**, whose pseudo-diequatorial diol functions reside essentially on the flat aromatic plane (Figure 9a). This means that **3** would have a sterically and electrostatically better affinity for the minor groove, thereby yielding greater amounts of dG adducts than the anti-isomer **2**. This argument appears to be substantiated by the fact that **2** binds better with dA (dA/dG ratio, 0.79) than the syn-

isomer **3** (0.56) when reacted with native calf-thymus DNA. The bulky nonplanar **5**, however, would have less affinity for the minor groove regardless of the type of diol conformation, but it is readily accommodated in the wider major groove (dA/dG = 1.41). The "diol argument" is also in good agreement with the previous observations that the higher dA/dG ratio observed for sterically hindered diolepoxydes is probably due to the greater reactivity of the planar ones for the amino group of dG residue, not to a greater affinity of the former for dA residues in DNA (18).

In general, the mutagenicity data seem to agree with the DNA binding profiles discussed above. The pseudo-diequatorial **2** is about seven times more potent than the pseudo-diaxial syn-isomer **3**, but is significantly less potent than the corresponding nonplanar analogue **5** (Figure 6) The mutation pattern is similar to that observed for the planar anti- and syn-chrysene-1,2-diol-3,4-epoxides, which also possess four benzene rings, but differ only in the fusing arrangement of the terminal benzene ring (9, 48). The mutagenicity testing results with the parent PAH in the presence of S9-mix activation system, however, seem to contrast with those obtained with the diolepoxydes derivatives (Figure 7). The markedly strong mutagenic activity of **1** as compared to **4** in this system is most likely due to the lack of metabolic activation of the latter. This finding is consistent with the enhanced tumorigenicity of chrysene relative to BcP (48).

In summary, we have characterized the structures of DNA adducts and tetraols derived from anti (**2**) (preceding paper)- and syn (**3**)-B[ghi]FDE (this paper). Both **2** and **3** gave deoxynucleoside adducts similar to those obtained from **5**, suggesting that the reactivities at the dibenzylic C5a are comparable to the benzylic cation of alternant (1, 2) and nonalternant (38, 49, 50) PAH diolepoxydes. The binding studies suggest that the nonplanar **5** reacts with cellular DNA differently than **2** and **3** due to differences in its structure and electronic configuration. Electronically, the puckered aromatic ring system results in less resonance stabilization of benzylic carbocation, allowing diolepoxydes to react better with DNA. Structurally, **5** is nonplanar, so that it preferentially binds to the wider major groove, where the exocyclic amino group of dA resides. On the other hand, planar diolepoxydes **2** and **3** are well accommodated into the minor groove, exhibiting relatively higher bindings to dG. The T-shaped pseudo-diaxial diol of **3** might have a favorable electrostatic interaction with the phosphate backbone of DNA, thus resulting in a greater reactivity to dG. "Docking" modeling studies are being carried out to better understand the nature of the diol-phosphate interaction prior to ring opening.

**Acknowledgment.** We wish to thank Dr. Peter Fu at NCTR for his helpful discussion and Ms. Suzy Von Tungeln for her help in acquiring CD spectra.

## References

- Harvey, R. G. (1996) Mechanisms of carcinogenesis of polycyclic aromatic hydrocarbons, *Polycyclic Aromat. Compd.* **9**, 1–23.
- Conney, A. H. (1982) Induction of microsomal enzymes by foreign chemicals and carcinogenesis by polycyclic aromatic hydrocarbons: G. H. A. Clowes Memorial Lecture. *Cancer Res.* **42**, 4875–4917.
- Geacintov, N. E., Cosman, M., Hingerty, B. E., Amin, S., Brody, S., and Patel, D. J. (1997) NMR solution structures of stereoisomeric covalent polycyclic aromatic carcinogen-DNA adducts: principles, patterns, and diversity. *Chem. Res. Toxicol.* **10**, 112–146.
- Dipple, A., Khan, Q. A., Page J. E., Ponten, I., and Szeliga, J. (1999) DNA reactions, mutagenic action and stealth properties of polycyclic hydrocarbon carcinogens (Review). *Intern. J. Oncol.* **14**, 103–111.
- Cavalieri, E. L., and Rogan, E. G. (1992) The approach to understanding aromatic hydrocarbon carcinogenesis; the central role of radical cations in metabolic activation. *Pharmacol. Ther.* **55**, 183–199.
- Buterin, T., Hess, M. T., Luneva, N., Geacintov, N. E., Amin, S., Kroth, H., Seidel, A., and Naegeli, H. (2000) Unrepaired fjord region polycyclic aromatic hydrocarbons-DNA adducts in ras codon 61 mutational hot spots. *Cancer Res.* **60**, 1849–1856.
- Sundberg, K., Widersten, M., Seidel, A., Mannervik, B., and Jernstrom, B. (1997) Glutathione conjugation of bay- and fjord-region diol epoxides of polycyclic aromatic hydrocarbons by glutathione transferases M1-1 and P1-1. *Chem. Res. Toxicol.* **10**, 1221–1227.
- Lin, C. H., Huang, X., Kolbanovskii, A., Hingerty, B. E., Amin, S., Brody, S., Geacintov, N. E., and Patel D. J. (2001) Molecular topology of polycyclic aromatic carcinogens determines DNA adduct conformation: a link to tumorigenic activity. *J. Mol. Biol.* **306**, 1059–80.
- Glatt, H., Pi e, A., Pauly, K., Steinbrecher, T., Schrode, R., Oesch, F., and Seidel, A. (1991) Fjord- and bay-region diol-epoxides investigated for stability, SOS induction in *Escherichia coli*, and mutagenicity in *Salmonella typhimurium* and mammalian cells. *Cancer Res.* **51**, 1659–1667.
- Phillips, D. H., Hewer, A., Seidel, A., Steinbrecher, T., Schrode, R., Oesch, F., and Glatt, H. (1991) Relationship between mutagenicity and DNA adduct formation in mammalian cells for fjord- and bay-region diol-epoxides of polycyclic aromatic hydrocarbons. *Chem.-Biol. Interactions* **80**, 177–186.
- Ralston, S. L., Seidel, A., Luch, A., Platt, K. L., and Baird, W. M. (1995) Stereoselective activation of dibenzo[a,h]pyrene to (–)-anti(11*R*, 12*S*, 13*S*, 14*R*)- and (+)-syn(11*S*, 12*R*, 13*S*, 14*R*)-11,12-diol-13,14-epoxides which bind extensively to deoxyadenosine residues of DNA in the human carcinoma cell line MCF-7. *Carcinogenesis* **15**, 2899–2907.
- Ralston, S. L., Coffing, S. L., Seidel, A., Luch, A., Platt, K. L., and Baird, W. M. (1997) Stereoselective activation of dibenzo[a,h]pyrene and its *trans*-11,12-dihydrodiol to fjord-region 11,12-diol-13,14-epoxides in a human mammary carcinoma MCF-7 cell-mediated V79 cell mutation assay. *Chem. Res. Toxicol.* **10**, 687–693.
- Amin, S., Desai, D., Dai, W., Harvey, R. G., and Hecht, S. S. (1995) Tumorigenicity in newborn mice of fjord-region and other sterically hindered diolepoxydes of benzo[*g*]chrysene, dibenzo[a,h]pyrene (dibenzo[*def,p*]chrysene), 4*H*-cyclopenta[*def*]chrysene and fluoranthene. *Carcinogenesis* **16**, 2813–2817.
- Luch, A., Glatt, H., Platt, K. L., Oesch, F., and Seidel, A. (1994) Synthesis and mutagenicity of the diastereomeric fjord-region 11,12-dihydrodiol 13,14-epoxides of dibenzo[a,h]pyrene. *Carcinogenesis* **15**, 2507–2516.
- Agarwal, R., Canella, K. A., Yagi, H., Jerina, D. M., and Dipple, A. (1996) Benzo[*c*]phenanthrene-DNA adducts in mouse epidermis in relation to the tumorigenicities of four configurationally isomeric 3,4-dihydrodiol 1,2-epoxides. *Chem. Res. Toxicol.* **9**, 586–592.
- Amin, S., Krzeminski, J., Rivenson, A., Kurtzke, C., Hecht, S. S. and El-Bayoumy, K. (1995) Mammary carcinogenicity in female CD rats of fjord region diolepoxydes of benzo[*c*]phenanthrene, benzo[*g*]chrysene and dibenzo[a,h]pyrene. *Carcinogenesis* **16**, 1971–1974.
- Vepachedu, S., Ya, N., Yagi, H., Sayer, J. M., and Jerina, D. (2000) Marked differences in base selectivity between DNA and the free nucleotides upon adduct formation from bay- and fjord-region diol epoxides. *Chem. Res. Toxicol.* **13**, 883–890.
- Szeliga, J., Amin, S., Zhang, F. J., and Harvey, R. G. (1999) Reactions of dihydrodiol epoxides of 5-methylchrysene and 5,6-dimethylchrysene with DNA and deoxyribonucleotides. *Chem. Res. Toxicol.* **12**, 347–352.
- Szeliga, J., and Dipple, A. (1998) DNA adduct formation by polycyclic aromatic hydrocarbon dihydrodiol epoxides. *Chem. Res. Toxicol.* **11**, 1–11.
- Chang, H.-F., and Cho, B. P. (1999) Synthesis of anti- and syn-diol epoxides of *trans*-3,4-dihydroxy-3,4-dihydrobenzo[*ghi*]fluoranthene: model planar diol epoxides. *J. Org. Chem.* **64**, 9051–9056.

- (21) Wise, S. A., Benner, B. A., Byrd, G. D., Chesler, S. N., Rebbert, R. E., and Schantz, M. M. (1988) Determination of polycyclic aromatic hydrocarbons in a coal tar standard reference material. *Anal. Chem.* **60**, 887–894.
- (22) Levin, W., Wood, A. W., Chang, R. L., Ittah, Y., Croisy-Delcey, M., Yagi, H., Jerina, D. M., and Conney, A. H. (1980) Exceptionally high tumor-initiating activity of benzo[*c*]phenanthrene bay-region diol-epoxides in mouse skin. *Cancer Res.* **40**, 3910–3914.
- (23) Sayer, J. M., Yagi, H., Croisy-Delcey, M., and Jerina, D. M. (1981) Novel bay-region diol-epoxides from benzo[*c*]phenanthrene. *J. Am. Chem. Soc.* **103**, 4970–4972.
- (24) Dipple, A., Pigott, M. A., Agarwal, S. K., Yagi, H., Sayer, J. M., and Jerina, D. M. (1987) Optically active benzo[*c*]phenanthrene diol-epoxides bind extensively to adenine in DNA. *Nature* **327**, 535–536.
- (25) Levin, W., Chang, R. L., Wood, A. W., Thakker, D. R., Yagi, H., Jerina, D. M., and Conney, A. H. (1986) Tumorigenicity of optical isomers of the diastereomeric bay-region 3,4-diol-1,2-epoxides of benzo[*c*]phenanthrene in murine tumor models. *Cancer Res.* **46**, 2257–2261.
- (26) Thakker, D. R., Levin, W., Yagi, H., Yeh, H. J. C., Ryan, D. E., Thomas, P. E., Conney, A. H., and Jerina, D. M. (1986) Stereoselective metabolism of the (+)-(*S,S*)- and (–)-(*R,R*)-enantiomers of *trans*-3,4-dihydroxy-3,4-dihydrobenzo[*c*]phenanthrene by rat and mouse liver microsomes and by a purified and reconstituted cytochrome P-450 system. *J. Biol. Chem.* **261**, 5404–5413.
- (27) Agarwal, S. K., Sayer, J. M., Yeh, H. J. C., Pannell, L. K., Hilton, B. D., Pigott, M. A., Dipple, A., Yagi, H., and Jerina, D. M. (1987) Chemical characterization of DNA adducts derived from the configurationally isomeric benzo[*c*]phenanthrene-3,4-diol 1,2-epoxides. *J. Am. Chem. Soc.* **109**, 2497–2504.
- (28) Amin, S., Desai, D., and Hecht, S. S. (1993) Tumor-initiating activity on mouse skin of bay-region diol-epoxides of 5,6-dimethyl and benzo[*c*]phenanthrene. *Carcinogenesis* **14**, 2033–2037.
- (29) Wood, A. W., Chang, R. L., Levin, W., Thakker, D. R., Yagi, H., Sayer, J. M., Jerina, D. M., and Conney, A. H. (1984) Mutagenicity of the enantiomers of the diastereomeric bay-region benzo[*c*]phenanthrene 3,4-diol-1,2-epoxides in bacterial and mammalian cells. *Cancer Res.* **44**, 2320–2324.
- (30) Bigger, C. A. H., St. John, J., Yagi, H., Jerina, D. M., and Dipple, A. (1992) Mutagenic specificities of four stereoisomeric benzo[*c*]phenanthrene dihydrodiol epoxides. *Proc. Natl. Acad. Sci. U.S.A.* **89**, 368–372.
- (31) U.S. PHS, National Institutes of Health, *Survey of compounds which have been tested for carcinogenic activity*, PHS Publication No. 149, National Cancer Institute, NIH, PHS, 1970–1971 Volume, p 446.
- (32) *NIH Guidelines for the Laboratory Use of Chemical Carcinogens* (1981) NIH Publication 81-2385, U.S. Government Printing Office, Washington, D. C.
- (33) Chiarelli, M. P., Gu, X., Aldridge, A. A., and Wu, H. (1998) Matrix-assisted laser desorption ionization and time-of-flight mass spectrometry for the sensitive determination of arylamide-deoxy-nucleoside adducts. *Anal. Chim. Acta* **368**, 1–9.
- (34) Huffer, D. M., Chang, H.-F., Cho, B. P., Zhang, L., and Chiarelli, M. P. (2001) Product ion studies of diastereomeric benzo[*ghi*]fluoranthene tetraols by matrix-assisted laser desorption ionization time-of-flight mass spectrometry and post-source decay. *J. Am. Soc. Mass Spectrom.* **12**, 376–380.
- (35) Maron, D. M., and Ames, B. N. (1983) Revised methods for the *Salmonella* mutagenicity test. *Mutat. Res.* **113**, 173–215.
- (36) Cheh, A. M., Chadha, A., Sayer, J. M., Yeh, H. J. C., Yagi, H., Pannell, L. K., and Jerina, D. M. (1993) Structures of covalent nucleoside adducts formed from adenine, guanine, and cytosine bases of DNA and the optically active bay-region 3,4-diol 1,2-epoxides of benz[*a*]anthracene. *J. Org. Chem.* **58**, 4013–4022.
- (37) Chadah, A., Sayer, J. M., Yeh, H. J. C., Yagi, H., Cheh, A. M., Pannell, L. K., and Jerina, D. M. (1989) Structures of covalent nucleoside adducts formed from adenine, guanine, and cytosine bases in DNA and the optically active bay-region 3,4-diol 1,2-epoxides of dibenz[*a,j*]anthracene. *J. Am. Chem. Soc.* **111**, 5456–5463.
- (38) Day, B. W., Sahali, Y., Hutchins, D. A., Wildschütte, M., Pastorelli, R., Nguyen, T. T., Naylor, S., Skipper, P. L., Wishnok, J. S., and Tannenbaum, S. R. (1992) Fluoranthene metabolism: human and rat liver microsomes display different stereoselective formation of the *trans*-2,3-dihydrodiol. *Chem. Res. Toxicol.* **5**, 779–786.
- (39) Dipple, A. (1988) Reactive metabolites of carcinogens and their interaction with DNA. In *Chemical Carcinogens: Activation Mechanisms, Structural, Electronic Factors, and Reactivity, Bioactive Molecules* (Politzer, E., Martin, F. J., Jr., Eds.) Vol. 5, pp 32–63, Elsevier, New York.
- (40) Szeliga, J., Page, J. E., Hilton, B. D., Kiselyov, A. S., Harvey, R. G., Dunayevsky, Y. M., Vouros, P., and Dipple, A. (1995) Characterization of DNA adducts formed by *syn*-benzo[*g*]chrysene 11,12-dihydrodiol 13,14-epoxide. *Chem. Res. Toxicol.* **8**, 1014–1019.
- (41) Szeliga, J., Lee, H., Harvey, R. G., Page, J. E., Ross, H. L., Routledge, M. N., Hilton, B. D., and Dipple, A. (1994) Reaction with DNA and mutagenic specificity for *syn*-Benzo[*g*]chrysene 11,12-Dihydrodiol 13,14-Epoxide. *Chem. Res. Toxicol.* **7**, 420–427.
- (42) Agarwal, R., Yagi, H., Jerina, D. M., and Dipple, A. (1996) Benzo[*c*]phenanthrene 3,4-dihydrodiol 1,2-epoxide adducts in native and denatured DNA. *Carcinogenesis* **17**, 1773–1776.
- (43) Lewis-Bevan, L., Little, S. B., and Rabinowitz, J. R. (1995) Quantum mechanical studies of the structure and reactivities of the diol epoxides of benzo[*c*]phenanthrene. *Chem. Res. Toxicol.* **8**, 499–505.
- (44) *Current Protocols in Nucleic Acid Chemistry* (2000) Vol. 1, Wiley, New York.
- (45) Cosman, M., Fiala, R., Hingerty, B. E., Laryea, A., Lee, H., Harver, R. G., Amin, S., Geacintov, N. E., Broyde, S., and Patel, D. J. (1995) Solution conformation of the (+)-*trans-anti*-[BPh]dA adduct opposite dT in a DNA duplex: interaction of the covalently attached benzo[*c*]phenanthrenyl ring to the 5'-side of the adduct site without disruption of the modified base pair. *Biochemistry* **32**, 12488–12497.
- (46) Cosman, M., Laryea, A., Fiala, R., Hingerty, B. E., Amin, S., Geacintov, N. E., Broyde, S., and Patel, D. J. (1995) Solution conformation of the (–)-*trans-anti*-Benzo[*c*]phenanthrene-dA ([BPh]-dA) adduct opposite dT in a DNA duplex: interaction of the covalently attached benzo[*c*]phenanthrenyl ring to the 3'-side of the adduct site and comparison with the (+)-*trans-anti*-[BPh]dA opposite dT stereoisomer. *Biochemistry* **34**, 1295–1307.
- (47) Suri, A. F., Mao, B., Amin, S., Geacintov, N. E., and Patel, D. J. (1999) Solution conformation of the (+)-*trans-anti*-benzo[*g*]chrysene-dA adduct opposite dT in a DNA duplex. *Biochemistry* **38**, 289–307.
- (48) Wood, A. W., Chang, R. L., Levin, W., Ryan, D. E., Thomas, P. E., Croisy-Delcey, M., Ittah, Y., Yagi, H., Jerina, D. M., and Conney, A. H. (1980) Mutagenicity of the dihydrodiols and bay-region diol-epoxides of benzo[*c*]phenanthrene in bacterial and mammalian cells. *Cancer Res.* **40**, 2878–2883.
- (49) Babson, J. R., Russo-Rodriguez, S. E., Rastetter, W. H., and Wogan, G. N. (1986) *In vitro* DNA-binding of microsomally-activated fluoranthene: evidence that the major product is a fluoranthene N<sup>2</sup>-deoxyguanosine adduct. *Carcinogenesis* **7**, 859–865.
- (50) Weyand, E. H., Bryla, P., Wu, Y., He, Z.-M., LaVoie, E. J. (1993) Detection of the major DNA Adducts of benzo[*j*]fluoranthene in mouse skin: nonclassical dihydrodiol epoxides. *Chem. Res. Toxicol.* **6**, 117–124.

TX0101346